Low-Threshold Exocytosis Induced by cAMP-Recruited $Ca_V3.2$ (α_{1H}) Channels in Rat Chromaffin Cells

A. Giancippoli, M. Novara, A. de Luca, P. Baldelli, A. Marcantoni, E. Carbone, and V. Carabelli
Department of Neuroscience, NIS Centre of Excellence, CNISM Research Unit, 10125 Turin, Italy

ABSTRACT We have studied the functional role of Ca_V3 channels in triggering fast exocytosis in rat chromaffin cells (RCCs). Ca_V3 T-type channels were selectively recruited by chronic exposures to cAMP (3 days) via an exchange protein directly activated by cAMP (Epac)-mediated pathway. Here we show that cAMP-treated cells had increased secretory responses, which could be evoked even at very low depolarizations (–50, –40 mV). Potentiation of exocytosis in cAMP-treated cells did not occur in the presence of 50 μM Ni^{2+}, which selectively blocks T-type currents in RCCs. This suggests that the "low-threshold exocytosis" induced by cAMP is due to increased Ca^{2+} influx through cAMP-recruited T-type channels, rather than to an enhanced secretion downstream of Ca^{2+} entry, as previously reported for short-term cAMP treatments (20 min). Newly recruited T-type channels increase the fast secretory response at low voltages without altering the size of the immediately releasable pool. They also preserve the Ca^{2+} dependence of exocytosis, the initial speed of vesicle depletion, and the mean quantal size of single secretory events. All this indicates that cAMP-recruited Ca_V3 channels enhance the secretory activity of RCCs at low voltages by coupling to the secretory apparatus with a Ca^{2+} efficacy similar to that of already existing high-threshold Ca^{2+} channels. Finally, using RT-PCRs we found that the fast inactivating low-threshold Ca^{2+} current component recruited by cAMP is selectively associated to the α_{1H} ($Ca_V3.2$) channel isoform.

INTRODUCTION

Regulated exocytosis in chromaffin cells is mainly controlled by Ca_V1 and Ca_V2 voltage-gated Ca^{2+} channels even though their expression varies among animal species and their coupling to secretion remains controversial (1–9). Several reports indicate that exocytosis is preferentially controlled by Ca_V1 (L-type), $Ca_V2.1$ (P/Q-type), or $Ca_V2.3$ (R-types) (8,10–12), suggesting specific colocalization of Ca^{2+} channels to secretory sites. Alternatively, other works favor the idea that Ca^{2+} channels contribute equally to exocytosis, depending on their density and contribution to the overall Ca^{2+} current (13–18). In particular, release depends on the total Ca^{2+} charge entering the cell and on the filling state of the readily releasable pool (RRP) (19,20). There is also evidence that whereas in spherical chromaffin cells secretion is randomly distributed, in neurite-emitting chromaffin cells, vesicles and clusters of P/Q-type channels are colocalized at the release sites of neurite terminals and L-type channels are uniformly distributed (21).

Besides these controversies, very little is known about the expression of functional T-type channels and their coupling to secretion in chromaffin cells. T-type channels are expressed in bovine chromaffin cells (BCCs) (22), in immature rat chromaffin cells (RCCs) (23), and in a small percentage of adult RCCs (24). Recently, we have shown that in most RCCs, 3–5 days exposure to pCPT-cAMP induces the expression of Ca_V3 channels without altering the proportions of other Ca^{2+} channels (25). This long-term action of cAMP clearly has different consequences with respect to the short-term effects (1 mM, 30 min), which cause upregulation of L-type channel gating and marked increase of secretion downstream of the Ca^{2+} entry (14,26,27). Thus, prolonged exposures to pCPT-cAMP appear useful for studying whether newly synthesized T-type channels are effectively coupled to catecholamine secretion in RCCs.

To date there are few reports suggesting a role of T-type channels in neurosecretion. T-type channels sustain the secretion of aldosterone in the adrenal glomerulosa (28), control insulin release in INS-1 β-cells (29) and the release of atrial natriuretic factor in rat cardiomyocytes (30), and mediate fast exocytosis in melanotropes (31), retinal bipolar cells (32), and mouse pheochromocytoma cell lines (MPC 9/3L) (33). In immature RCCs, T-type channels contribute markedly to the total Ca^{2+} current but fail to produce secretion (23). This suggests that either their activation-secretion coupling requires some critical element that is missing during development or, alternatively, they are located apart from release sites contradicting the observation that secretion in adult RCCs occurs regardless of the type of functioning Ca^{2+} channels (14). To solve these issues, we raised the question whether cAMP-recruited T-type channels are involved in depolarization-evoked exocytosis and how they are possibly coupled to the exocytic machinery in adult RCCs.

Here, we show that long-term exposures to cAMP uniquely recruit the $Ca_V3.2$ (α_{1H}) channel isoform uncovering a ''low-threshold'' secretory response that is normally absent in control RCCs. The cAMP-enhanced secretion exhibits the typical sensitivity to Ni^{2+} of $Ca_V3.2$ T-type

Submitted July 29, 2005, and accepted for publication November 29, 2005.

Address reprint requests to Emilio Carbone, Dept. of Neuroscience, Corso Raffaello 30, 10125 Turin, Italy. Tel.: 39-011-670-7786; Fax: 39-011-670-7708; E-mail: emilio.carbone@unito.it.

P. Baldelli's present address is Dept. of Experimental Medicine, Viale Benedetto XV, 3 I-16100 Genoa, Italy.

0006-3495/06/03/1830/12 $2.00

doi: 10.1529/biophysj.105.071647

channels and is absent when either L or R are the only Ca^{2+} channels available. This suggests strict correlation to the Ca^{2+} influx through T-type channels, rather than an effect on the secretory machinery downstream of Ca^{2+} entry. The ''low-threshold'' potentiation of exocytosis by cAMP treatment was mainly associated with an increased Ca^{2+} charge recruited at negative potentials and preserved the size of the immediately releasable pool (IRP) mobilized by short depolarizations, the Ca^{2+} dependence of exocytosis and the quantal size of single secretory events. Thus, cAMP-recruited $Ca_V3.2$ channels appear effectively coupled to the secretory apparatus and control fast exocytosis in a way comparable to Ca_V1 and Ca_V2 channels.

MATERIALS AND METHODS

Isolation and culture of rat chromaffin cells

Chromaffin cells were obtained from the adrenal glands of adult Sprague Dawley rats (200–300 g) as previously described (14). All experiments were carried out in accordance with the guidelines established by the National Council on Animal Care and were approved by the local Animal Care Committee of Turin University. Before cell plating, plastic dishes were pretreated with poli-L-ornithine (1 mg/ml) and laminin (5 μg/ml in L-15 carbonate) for improving cell adhesion. Cells were then cultured at 37°C in a water-saturated atmosphere with 5% CO_2. Culture medium contained Dulbecco's modified Eagle's medium, penicillin-streptomycin 0.5%, and gentamycin 0.25%, was serum-free, and was not changed during the culture period. After 24 h since their plating, cells were exposed to the membrane permeable cAMP analog pCPT-cAMP (200 μM) and then maintained up to 5 days (4 days with cAMP) in the culture medium (25).

RNA extraction and reverse transcription-polymerase chain reaction

Total RNA was isolated from both control and 3 days cAMP-treated chromaffin cells with the RNeasy Micro Kit (Qiagen; AG, Basel, Switzerland) as indicated in the manufacturer's instructions. The cDNA was synthesized from 0.5 μg of DNase-treated total RNA in a total volume of 20 μl with the SuperScript First-Strand Synthesis System for RT-PCR (Life Technologies; Carlsbad, CA). RT-PCR experiments were carried out in a total volume of 25 μl, containing 10 μl of cDNA, 0.5 units of high-fidelity DNA polymerase, 5X Phusion GC buffer, 0.2% DMSO (Finnzymes, Espoo, Finland), and 0.2 mM of each deoxynucleotide triphosphate (Life Technologies) and 0.5 μM specific primer set. The primer sequences used were for α_1H (AF290213): 5′-GACGAGGATAAGACGTCT-3′ and 5′-AGGAGACGCGTAGCCT-GTT-3′; for α_1G (AF290212): 5′-TCAGAGCCTGATTTCTTT-3′ and 5′-CAGGAGACGAAACCTTGA-3′; for α1I (AF290214): 5′-GATGAG-GACCAGA GCTCA-3′ and 5′-CAGGATCCGGAACTTGTT-3′; for β-actin (NM_031144) 5′-GGACCTGACAGACTACCTCA-3′ and 5′-ATCTTGAT-CTTCATGGTGCT-3′; for dopamine β-hydroxilase (DBH; NM_013158) 5′-CCTTGAAGGGACTTTAGAGC-3′ and 5′-AGCAGCTGGTAGTCCT-GATG-3′. The cycling conditions were 98°C for 30 s, followed by 26 cycles of 98°C for 15 s, either 58°C (for α_1H, β-actin, and DBH) or 64°C (α_1G and α_1I) for 30 s and 72°C for 30 s. Positive (cDNA obtained from rat cerebellum total RNA) and negative (water instead of template) controls were amplified in the same conditions. The PCR product was run on 1.2% agarose gel stained with Gel Star (Cambrex; East Rutherford, NJ) in the presence of a 100 bp DNA ladder as the molecular weight marker (Promega; Madison, WI). The intensity of α1H, DBH, and β-actin bands was measured using dedicated software (ImageJ 1.33u). To minimize intrinsic variation, results were normalized to the amount of β-actin expression. All samples were tested simultaneously for the different primer sets.

Electrophysiological recordings

Ca^{2+} currents and capacitance increases were measured in the perforated-patch configuration by means of an EPC-9 patch-clamp amplifier (Heka-Electronic; Lambrecht, Germany) and PULSE software. Patch-clamp pipettes were fabricated from thin Kimax borosilicate glass (Witz Scientific; Holland, OH) and fire-polished to obtain a final series resistance of 2–3 MΩ.

Recordings started when the access resistance was below 15 MΩ, ~10 min after sealing (34). Ca^{2+} currents were sampled at 10 kHz and filtered at 2 kHz. The holding potential (Vh) was kept at –80 mV, and test depolarizations (10–200 ms) varied from –50 to +40 mV, except when otherwise indicated. The quantity of charge Q was evaluated as the time integral of the inward Ca^{2+} current. Exocytosis was estimated by means of capacitance increments (ΔC) by applying sinusoidal wave functions ($\pm$25 mV, 1 KHz) as previously described (14). Capacitance increments due to activation of voltage-gated Ca^{2+} channels were acquired at high time resolution using ''PULSE'' software, whereas at time intervals between step depolarizations, capacitance data were recorded at low time resolution using the X-Chart plug-in module of ''PULSE''. To determine the ΔC increment, membrane capacitance was averaged over 50 ms preceding the depolarization to give a reference value; this was subtracted from the value estimated after the depolarization, averaged over a 400 ms window, excluding the first 50 ms to avoid contamination by nonsecretory capacitative transients. Experiments were carried out at room temperature (22–24°C). Data are given as mean $\pm$ SE for n = number of cells. Statistical significance was calculated using unpaired Student's t-test, and p values <0.05 were considered significant. Fast capacitative transients during step depolarization were minimized online by the patch-clamp analog compensation. Currents were not corrected for leakage, and for this reason cells with leakage currents >15 pA at Vh were excluded from the analysis.

Solutions

The extracellular solution contained (mM) 145 TEACl, 5 $CaCl_2$, 10 glucose, 10 HEPES (pH 7.4 with CsOH). Except where otherwise specified, cells were incubated 15 min before recordings with ω-conotoxin-GVIA (3.2 μM) and ω-agatoxin-IVA (2 μM) (Scientific Marketing Associates; Barnet, UK) into an extracellular solution containing 2 mM instead of 5 mM $CaCl_2$.

Amphotericin B (Sigma, St. Louis, MO) was used to achieve the perforated patch configuration (14). Amphotericin B was dissolved in dimethyl sulfoxide (DMSO) and stocked at –20°C in aliquots of 50 mg/ml. The pipette-filling solution contained (mM): 135 $CsMeSO_3$, 8 NaCl, 2 $MgCl_2$, 20 HEPES, and 50–100 μg/ml amphotericin B (pH 7.3 with CsOH).

Series resistance was compensated by 80% and monitored during the experiment. Since the drugs applied to the external solution did not affect the liquid junction potential (LJP), the indicated voltages were not corrected for the LJP at the interface between the pipette solution (135 mM $CsMeSO_3$) and the bath (5 mM Ca^{2+} and 145 mM TEACl), which was 24.5 mV (35). Compared to previous measurements in whole-cell clamp recordings in 10 mM Ca^{2+} and 137 mM TRIS-HCl (LJP = 13.6 mV) (25), the voltage bias was ~10 mV more positive. However, since 5 mM Ca^{2+} induces an ~8 mV negative shift of voltage-dependent parameters with respect to 10 mM Ca^{2+}, these recordings are comparable to those previously reported by Novara et al. (25).

RESULTS

Long-term exposures to pCPT-cAMP selectively potentiate the expression of the α_{1H} mRNA subunit in RCCs

We have recently shown that 3–5 days exposure to the membrane permeable cAMP analog pCPT-cAMP (200 μM)

induces the recruitment of T-type channels in RCCs, which are not usually expressed in these cells (25). The fast inactivation kinetics (τ_{inact} 18–20 ms at +10 mV) and the high sensitivity to Ni^{2+} block (IC_{50} 16 μM in 10 mM Ca^{2+}) suggested that the cAMP-recruited T-type currents were most likely associated with the $Ca_V3.2$ channel isoform (36,37). To verify this, we ran a series of RT-PCRs aimed at identifying the molecular isoform involved.

RT-PCRs with primers against α_{1G}, α_{1H}, and α_{1I} subunits of Ca_v3 T-type channels were performed on total RNA from RCCs. We compared the subunit's expression level between control and 3 days cAMP-treated cells by applying non-saturating PCR conditions. In addition, we used primers for DBH and for the housekeeping gene β-actin to evaluate RNA integrity (Fig. 1, *A–C*). DBH was used since it is specifically expressed by chromaffin cells and upregulated by cAMP (38). RT-PCRs with primers against α_{1G} and α_{1I} revealed no messengers in control and cAMP-treated cells, whereas positive controls gave the expected products (Fig. 1, *B* and *C*). In contrast, in cAMP-treated cells we found marked expression of both the α_{1H} subunit and DBH mRNA, even though a smaller constitutive expression of the subunit was also found in cAMP-untreated cells (Fig. 1 *A*). This agrees with the observations that a small percentage of control cells (<10%) exhibited sizeable low-threshold currents. In addition, semiquantitative RT-PCR analysis indicated a 3.5-fold increase of α_{1H} expression after cAMP treatment (see Materials and Methods). Taken together, our results suggest that long-term incubations with cAMP selectively enhance the level of α_{1H} mRNA.

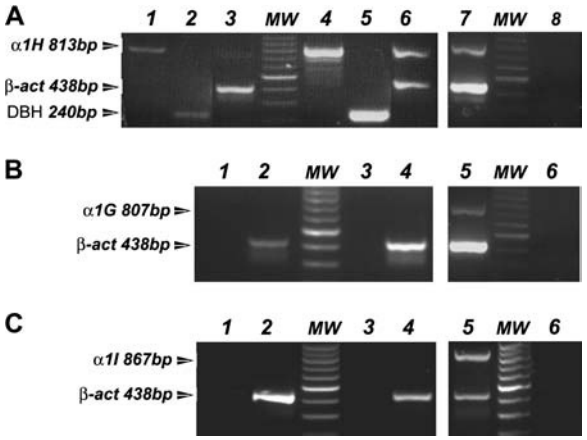

FIGURE 1 Differential expression of α_{1H} calcium channel subunit mRNA in control and cAMP-treated RCCs. Total RNA (0.5 μg) from adult RCCs was retrotranscribed and amplified with specific oligonucleotides (0.5 μM) for α_{1H}, α_{1G}, α_{1I}, DBH, and β-actin. (*A*) Upregulation of α_{1H} T-type channel after long-term cAMP treatment. PCR products for α_{1H} (lanes *1* and *4*), for DBH (lanes *2* and *5*) and α_{1H} plus β-actin (lanes *3* and *6*). Control cells are in lanes *1–3* and cAMP-treated cells in lanes *4–6*. mRNA from the entire rat brain is used as positive control (lane *7*). cDNA replaced with water is used as a negative control (lane *8*). (*B* and *C*) The α_{1G} and α_{1I} subunits are not expressed in control and in cAMP-treated RCCs. The PCR products for α_{1G} and α_{1I} (lanes *1* and *3*), α_{1G} plus β-actin, and α_{1I} plus β-actin (lanes *2* and *4*) are shown in control (lanes *1* and *2*) and cAMP-treated cells (lanes *3* and *4*). Positive and negative controls for the reaction are the mRNA from entire rat brain (lane *5*) and replacement of cDNA with water (lane *6*). PCR products were separated in 1.2% agarose gel in the presence of 100 bp DNA ladder (lane *MW*).

Exocytosis associated with T-type channels in cAMP-treated RCCs

To focus on the secretory responses evoked by T-type currents, N-, P/Q-, and L-type channels were blocked by pretreating the RCCs with mixtures of ω-CTx-GVIA (3.2 μM) and ω-Aga-IVA (2 μM) for 15 min before the experiment and by adding 1 μM nifedipine to the external solution. Attempts to block the R-type channels using the selective blocker SNX-482 (39) failed due to the insensitivity of Ca^{2+} currents to high concentrations of the toxin (0.1–1 μM) (25). Thus, our recordings mainly contained R-type currents in control conditions and mixtures of T- and R-type currents in cAMP-treated cells. In control RCCs the R-type current started activating above –30 mV, had fast activation, relatively slow inactivation kinetics (Figs. 2 *A* and 3 *A*), and in most cells (90%, $n = 25$) the current-voltage (I/V) relationship had a single negative peak around +10 mV (Fig. 2 *B*). In the remaining 10% of cells, T-type currents could also be detected at very negative potentials. These

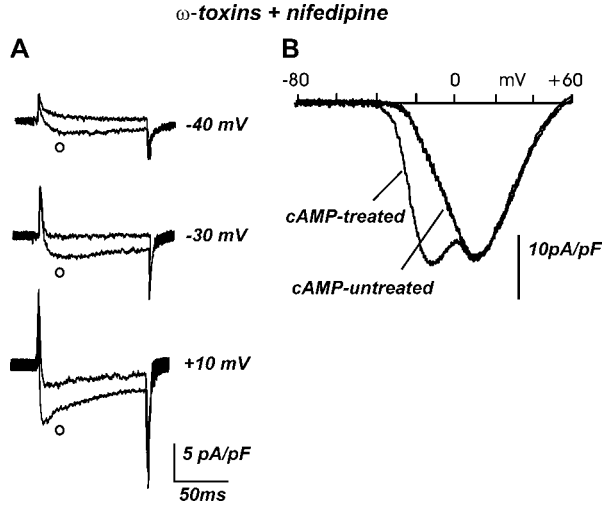

FIGURE 2 Low-threshold Ca^{2+} current upregulation by long-term cAMP treatment. (*A*) Comparison of representative Ca^{2+} currents in control cells and after long-term exposure to pCPT-cAMP (○). Depolarizations at –40, –30, and +10 mV from –80 mV holding potential. Cells were previously incubated with ω-CTx-GVIa (3.2 μM) and ω-Aga-IVa (2 μM); nifedipine (1 μM) was kept in the external solution. After cAMP treatment, Ca^{2+} currents are already detectable at –40 mV and become more rapidly inactivating at higher potentials. (*B*) The low-threshold component is more evident when applying a ramp command (from –80 mV to +60 mV), which produces an early peak at ~–15 mV.

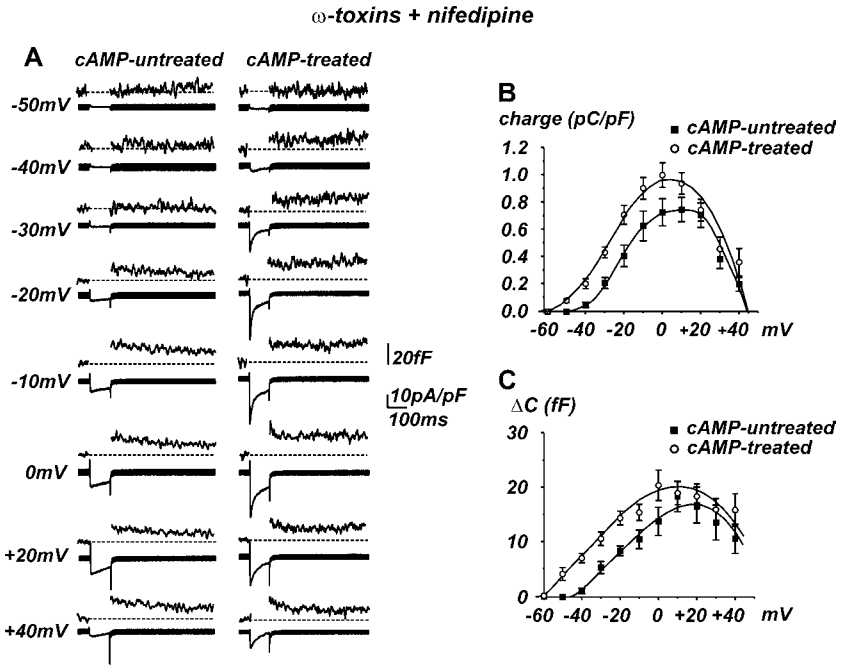

FIGURE 3 Long-term cAMP treatment potentiates the quantity of charge and secretion at low voltages. (*A*) Ca^{2+} currents and depolarization-evoked secretory responses for a control cell (*left*) and after long-term incubation with pCPT-cAMP (*right*). Cells were incubated with ω-toxins and nifedipine was in the bath. (*B*) Quantity of charge is calculated as the time integral of the current entering during the 100 ms depolarization; data are averaged from 25 cAMP-untreated (■) and 69 cAMP-treated cells (○), respectively. Experimental data were fitted to polynomial functions. (*C*) The corresponding secretion was measured by means of ΔC increases at the potentials indicated and plotted versus voltage.

RCCs, however, were not included in the statistics of control cells. In cAMP-treated cells, Ca^{2+} currents started activating at more negative potentials (–40 mV), had fast activation and rapid inactivation, and showed I/V curves with a second ''peak'' at ~–20 mV (87%, $n = 79$), confirming that in cAMP-treated RCCs T-type currents coexisted with R-type currents (Figs. 2 *A* and 3 *A*).

Having shown that cAMP selectively recruits α_{1H} T-type channel subunits, we next measured their associated exocytosis. Step depolarizations lasting 100 ms were applied from –50 mV to +40 mV. With respect to previous studies (14), we reduced the extracellular [Ca^{2+}] (from 10 to 5 mM) and replaced Na^+ with TEA^+ to minimize Na^+ inward currents. Replacement of Na^+ with TEA^+ was preferred to the addition of tetrodotoxin due to the slowing-down of Na^+ gating currents by the toxin (40). On the other hand, block of transient inward Na^+ currents was crucial for the correct estimate of the total Ca^{2+} charge associated with cAMP-recruited T-type channels. External solutions containing TEA^+ did not significantly alter the T-type current density and secretion. In fact 1), the density of T-type currents (25) and the secretion associated with various Ca^{2+} channels were comparable to those reported in Na^+ containing solutions. In 10 mM Ca^{2+} and 135 mM Na^+, a charge density of 1.7 pC/pF carried by L- and R-type channels produces a mean ΔC of 24 fF at +10 mV (14), which compares well with the 15 fF capacity change induced by 1.0 pC/pF through the same channels in 5 mM Ca^{2+} and 145 mM TEA^+ (see Fig. 6 *A*). 2), During the experiments, the RCCs were clamped to –80 mV, and in the short period preceding the clamping conditions (4–6 min) the secretion after TEA-induced depolarization was transient and lasted only 2–3 min, most likely because of Ca^{2+} channel inactivation (data not shown). We tested this by measuring the amperometric spikes associated to catecholamine secretion with carbon fiber microelectrodes.

As shown in Fig. 3, in control RCCs secretion started around –30 mV and reached maximal values at +10 mV (~17 fF $n = 25$, Fig. 3, *B* and *C*), in good agreement with the voltage dependence of Ca^{2+} charge, which started contributing around –30 mV and peaked at +10 mV. In most cAMP-treated RCCs' (87% of 79 cells) secretory responses could already be detected at very negative depolarization (–50, –40 mV). Exocytosis and quantity of charge were more prominent between –50 mV ($p < 0.01$) and –20 mV ($p < 0.05$), where T-type channels were activated and R-types contributed less (Fig. 3 *C*). Quantity of charge and capacitance increases reached maximal values at 0 mV (21 fF). Interestingly, the presence of T-type currents produced a broadening of both $Q(V)$ and $\Delta C(V)$ curves toward negative voltages rather than a second ''peak'' on the I/V characteristics (Fig. 2). This derives most likely from the peculiar voltage dependence of T-type channel gating, which produces sharp increases of the peak current between –40 and +10 mV followed by an increased rate of inactivation. The increased inactivation limits the quantity of Ca^{2+} charge flowing during pulses of 100 ms and produces weak voltage dependence of the $Q(V)$ curve associated with T-type channels. This is particularly evident between –30 and 0 mV, where the quantity of charge attributed to T-type channels is nearly unchanged, as can be inferred from the flat Q versus V relationship in cAMP-treated cells from –30 to 0 mV (Fig. 3, *B* and *C*). A similar weak voltage dependence is evident in the $\Delta C(V)$ curve.

Ni^{2+} blocks the low voltage-activated exocytosis associated with T-type current recruitment

Ni^{2+} is a potent blocker of $Ca_V3.2$ (α_{1H}) T-type channels (37) and is commonly used to separate T-types from residual high-voltage activated (HVA) currents, even though some R-type channel displays lower sensitivity to Ni^{2+} block (41). Fig. 4 *A* shows representative examples of the action of 50 μM Ni^{2+} (at –20 mV) on Ca^{2+} currents and exocytosis in cAMP-untreated and cAMP-treated cells. It is evident that Ni^{2+} exerted negligible effects in untreated cells, whereas it reduced the secretion by ~45% and abolished the fast inactivating currents in cAMP-treated RCCs. The most significant reduction of exocytosis in cAMP-treated cells was between –50 and –20 mV ($p < 0.05$, Fig. 4, *B* and *C*, *right panels*), whereas the effect was not significant in control RCCs ($p > 0.1$, *left panels*). Nevertheless, Ni^{2+} partially blocked the quantity of charge and secretion also in cAMP-untreated RCCs. This was more evident above +10 mV and attributed to a partial depression of residual R-type channels in control RCCs. Taken together, the results of Fig. 4 suggest that the ''low-threshold'' exocytosis associated with cAMP-recruited T-type channels exhibits the same sensitivity to Ni^{2+} of $Ca_V3.2$ channels.

Long-term cAMP treatment does not affect the density of R- and L-type currents and their related exocytosis

Having established that cAMP-recruited T-type channels produce sizable exocytosis (Figs. 2 and 3), we next investigated whether long-term cAMP treatments had any effect on the exocytosis associated to R and L types or whether they could affect the efficiency of the secretory apparatus. The latter occurs after brief applications (30 min), in which cAMP acts as an amplification factor for exocytosis regardless of the channel type carrying Ca^{2+} (14).

Fig. 5 shows that in ω-toxin-treated RCCs bathed in solutions containing 50 μM Ni^{2+} and 1 μM nifedipine to preserve only functionally active R-type channels, long-term treatments with cAMP preserve the density of charge and the associated secretion. The quantity of charge measured from –50 to +40 mV was the same in control ($n = 15$) and with cAMP ($n = 13$) ($p > 0.5$) (Fig. 5 *A*) and the same was true for the depolarization-evoked exocytosis, measured in the same voltage range (Fig. 5 *B*, $p > 0.5$). Thus, long treatments with cAMP seemed to affect neither the density of R-type channels nor the associated exocytosis (~13 fF between 0 and +20 mV), which nevertheless contributed to ~30% of the total secretion of RCCs, see Fig. 2 (14).

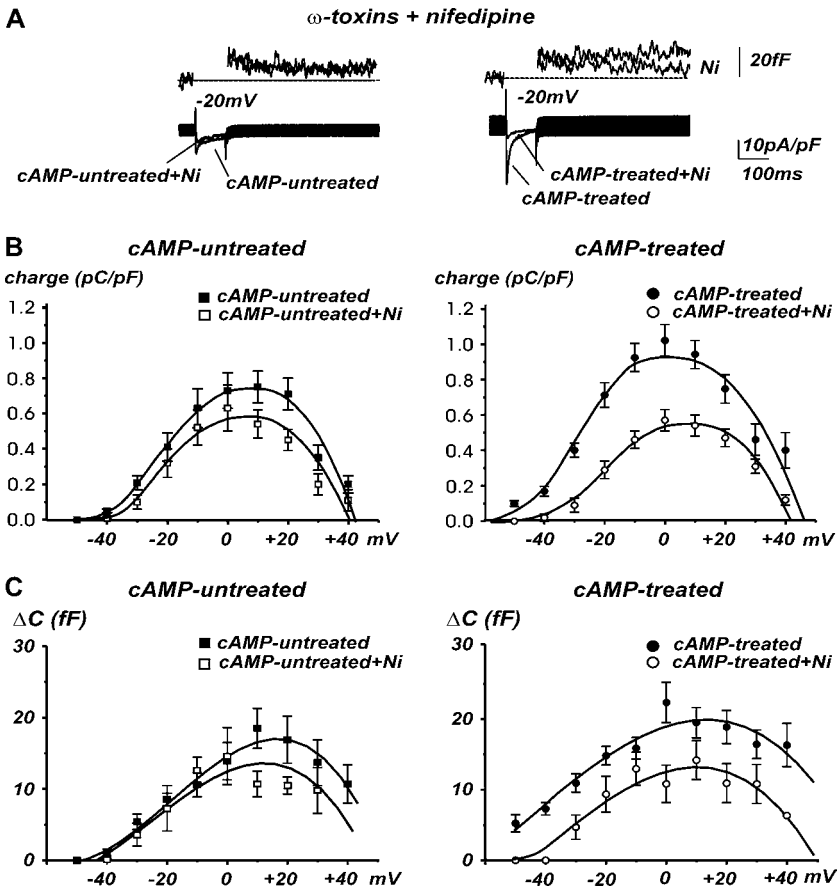

FIGURE 4 Quantity of charge and secretion recruited by cAMP is sensitive to Ni^{2+}. The T-type channel blocker Ni^{2+} (50 μM) has no effect on cAMP untreated cells, whereas it significantly reduces both Ca^{2+} currents and secretion after the long-term cAMP treatment. RCCs were pretreated with ω-toxins and nifedipine. (*A*) Representative traces for a cell depolarized at –20 mV. Left, cAMP-untreated cell; right, cAMP-treated cell. (*B* and *C*) Mean quantity of charge and mean secretory responses evaluated between –50 and +40 mV depolarizations. Ni^{2+} significantly reduced both the Ca^{2+} charge and the capacitance increases after cAMP treatment.

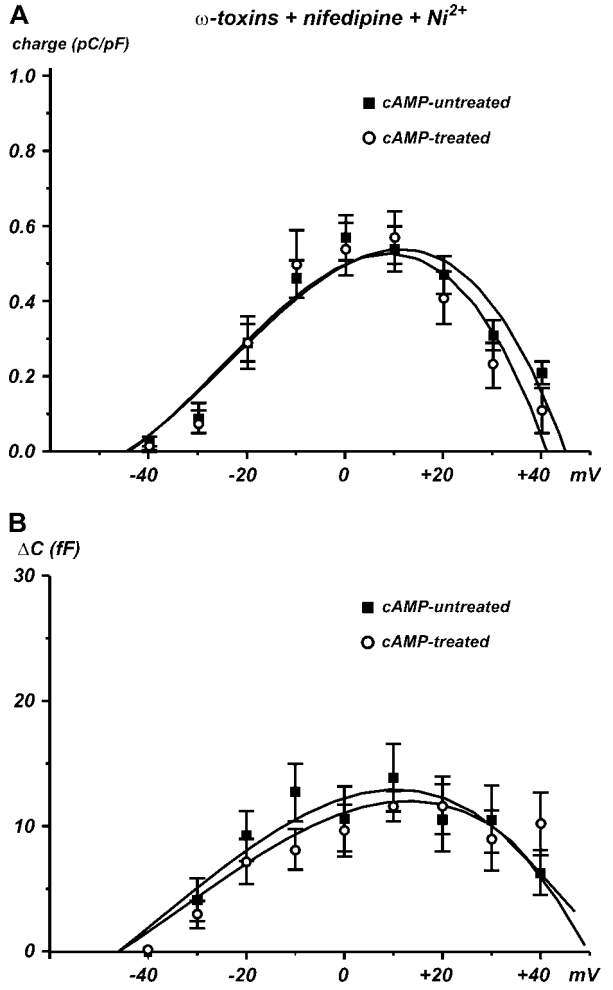

FIGURE 5 Long-term treatment with cAMP does not affect R-type currents and the related secretion. In the presence of ω-toxins, nifedipine, and Ni^{2+}, the long-term treatment with cAMP is ineffective in potentiating both the toxin-resistant R-type channels and the corresponding secretory response. Quantity of charge (*A*) and capacitance increases (*B*) were evaluated between –50 and +40 mV.

Similarly, long-term treatments with cAMP were ineffective on both exocytosis and quantity of charge when L- and R-type channels were available, i.e., in the presence of ω-toxins and Ni^{2+} in the bath (Fig. 6, *A* and *B*). L-type currents and the related exocytosis were evaluated at +10 mV using conditioning prepulses to –40 mV (14) to further inactivate the contribution of N- and P/Q-type channels, which could still function after washout of toxins. Test pulses lasted 120 ms to recruit the maximum number of vesicles from the IRP. In both cases, cAMP affected neither the quantity of charge nor the secretory response. After 120 ms pulses, the capacitance increase was 17.2 ± 3.3 fF (cAMP) versus 15.1 ± 1.4 fF (control) and the quantity of charge was 1.0 ± 0.2 pC/pF (cAMP, $n = 6$) versus 1.1 ± 0.3 pC/pF (control, $n = 10$). These results demonstrate that, as previously reported (25), the L-type current density also was insensitive to long-term cAMP treatments and that ~1.0 pC/pF of charge density induced ~15–17 fF secretion, independently of the presence of cAMP. Thus, we can conclude that the effects of 3 days cAMP treatment on exocytosis are primarily mediated by the expression of T-type channels and that the long-term treatment with cAMP is ineffective in potentiating exocytosis when either L-type or R-type are the only channels available.

Long-term exposure to cAMP preserves the size of the IRP and the Ca^{2+} dependence of exocytosis

Having established that T-type channels contribute to the fast secretory activity of RCCs at low voltages, we next studied the time course at which T-type channels contribute to the depletion of the IRP of vesicles that are mobilized during short depolarizations. We followed the method of Horrigan and Bookman (40) consisting of applying pulses of increasing duration to –20 mV and plotting ΔC versus pulse duration. As shown in Fig. 7, *A* and *B*, the T-type channel-induced secretion possesses the same kinetic features of that produced by HVA channels in RCCs (14,40): 1), the time course of the depolarization-evoked exocytosis is exponential ($\tau = 54$ ms) and is well fit by a first order kinetic model (*solid line*), 2), the initial rate of exocytosis (464 fF/s) estimated by fitting the two values at 10 and 20 ms decreases drastically at longer times, and 3), ΔC saturates with prolonged depolarization and the asymptote of the fit furnishes the size of IRP (21 fF). This value, however, should be considered an underestimate of the true IRP since saturation of ΔC was also reached, not only because of approaching complete mobilization of the IRP, but also because of the fast inactivation of T-type currents that limits the quantity of charge for pulses >100 ms.

To better estimate the size of the IRP in cAMP-treated and cAMP-untreated RCCs, we used a double-pulse protocol (42) that allowed maximal recovery of inactivated T-type channels after pulses of 100 ms at –30mV. Considering that recovery from fast inactivation of α_{1H} channels is almost complete in 1.5 s at –90 mV (43) and that refilling of the IRP proceeds at a rate 10 times slower ($\tau = 10$ s) (44), we used double pulses of 100 ms separated by interpulse intervals of 1.5 s (0.5 s at –80 mV for measuring ΔC and 1 s at –100 mV to fully recover T-type channels; Fig. 7 *C*, *bottom*). Since Ca^{2+} currents at –30 mV in cAMP-untreated cells were smaller with respect to cAMP-treated cells, the two pulses lasted longer in control cells (160 vs. 100 ms). In this way, all the assumptions of the method were satisfied to a great extent by 1), delivering pulses that mobilize a large fraction of the IRP, 2), injecting an equal quantity of charges at each pulse, and 3), causing minimal vesicle refilling during the two pulses. Fig. 7, *C* and *D*, shows that the lower and upper limits of the pool size (ΔC_1 and B_{max}) are not significantly different in control and after cAMP treatment: the mean B_{max} varies between 33.2 ± 5.2 fF and 36.8 ± 5.1 fF ($p < 0.5$) for cAMP-untreated and cAMP-treated cells. The same is true

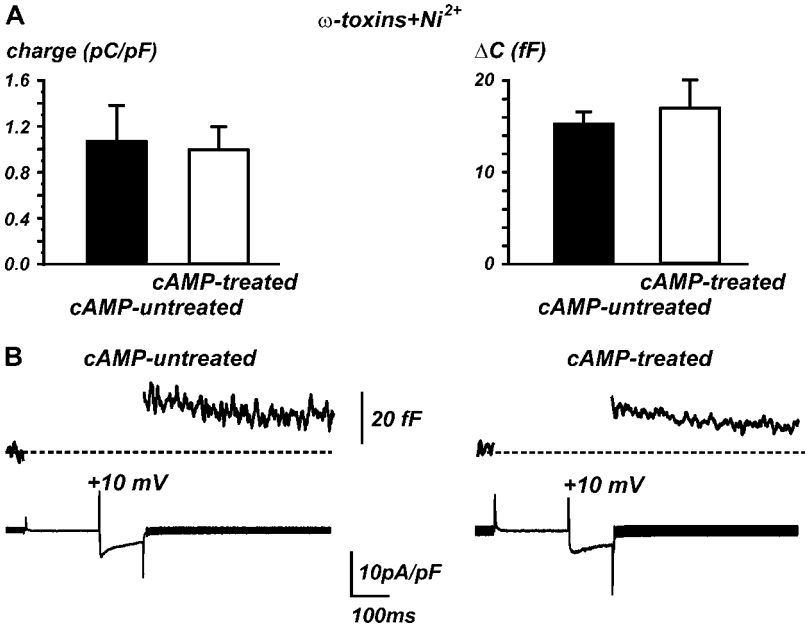

FIGURE 6 Long-term cAMP treatment does not alter L-type channel functionality and the related secretion. In sharp contrast to the action exerted on T-type channels, the long-term treatment with pCPT-cAMP failed to alter the functionality of nifedipine-sensitive L-type channels. (*A*) The charge entering during 120 ms depolarization at +10 mV and the depolarization-evoked secretion are not modified by cell incubation with pCPT-cAMP. (*B*) Representative traces of L-type currents and corresponding ΔC increases without and after cAMP treatment. To further inactivate N- and P/Q-type channels, a conditioning prepulse to –40 mV preceded the test depolarization (14).

for the ratio $\Delta C_2/\Delta C_1$ (0.34 ± 0.09 vs. 0.41 ± 0.07; $p < 0.5$), which furnishes the probability of vesicle release ($\Delta C_2/\Delta C_1 = 1 - p$). Thus, cAMP-recruited T-type channels do not alter the size of IRP and the probability of vesicle release. It is worth noticing, however, that during interpulse intervals of 1.5 s some degree (15%–20%) of vesicle refilling is likely to occur. This would produce increased values of ΔC_2 and a consequent overestimate of B_{max} that should be partially compensated by a 5%–10% physiological decrease of Ca^{2+} charge during the second pulse. These drawbacks, however, would affect equally the estimate of IRP of both cAMP-treated and -untreated cells (Fig. 7 *D*).

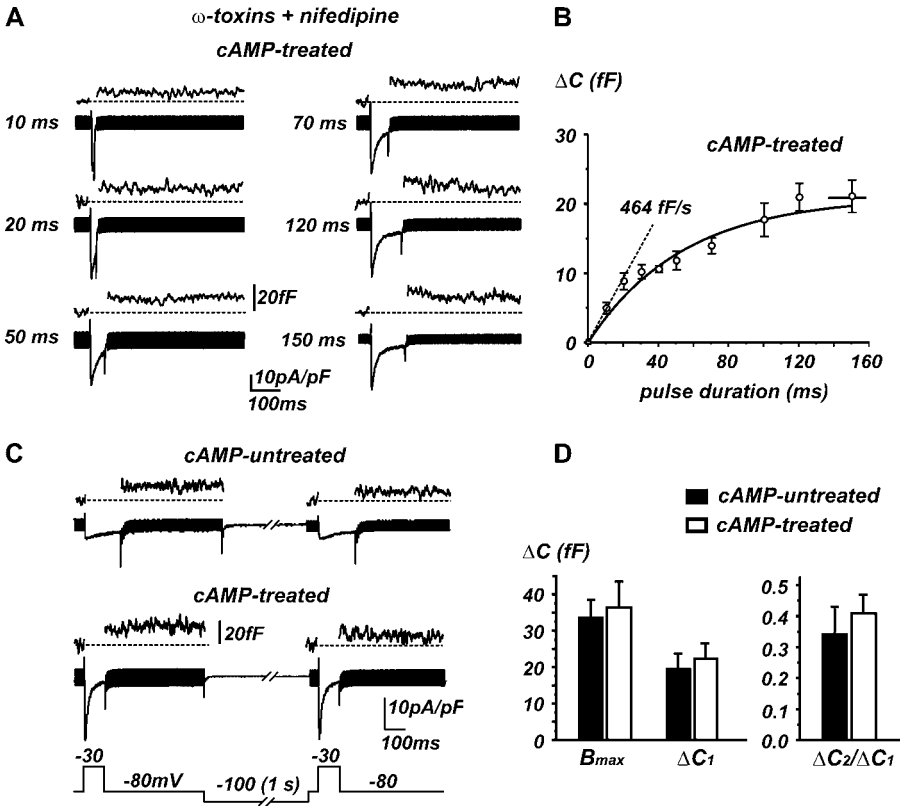

FIGURE 7 Size of the IRP is preserved by the long-term cAMP treatment. (*A*) RCCs were pretreated with ω-toxins and nifedipine, and depolarized with pulses of different length (from 10 to 150 ms) at –20 mV to evoke increasing secretion. (*B*) Plot of ΔC increases versus the corresponding pulse length; data are averaged from 20 cAMP-treated cells like the one tested in panel *A*. The solid curve is an exponential fit with $\tau = 54$ ms and maximal value indicated by the asymptote (21 fF). The dashed line drawn to fit the first two points at 10 and 20 ms has a slope of 464 fF/s and indicates the initial rate of exocytosis. (*C*) Double pulse protocol for estimating the IRP size. Two depolarizations at –30 mV were applied consecutively after a 1 s interval to −100 mV, as illustrated. Test pulses lasted 160 ms for cAMP-untreated and 100 ms for cAMP-treated cells to allow comparing the secretion induced by equal quantity of charges in both conditions. Each pair of depolarization was repeated at least three times, and values of ΔC were averaged for each cell. RCCs were not pretreated with ω-toxins and nifedipine. (*D*) Bar histograms indicate for cAMP-untreated (*solid bars*) and for cAMP-treated cells (*open bars*), respectively, the calculated values of B_{max} (IRP size) (24), the capacitance increment ΔC_1, and the ratio $\Delta C_2/\Delta C_1 = (1 - p)$, with p indicating the probability of release.

Finally, the Ca^{2+} dependence of exocytosis was evaluated by plotting the capacitance increases versus the corresponding quantity of charge (Fig. 8). As in BCCs (45) and other neuroendocrine cells (46), secretion in RCCs is roughly linearly related to the quantity of charge Q, particularly for small quantities of Ca^{2+} charges (<30 pC), as in our case (14,40). Linearity between Ca^{2+} entry and exocytosis was observed up to 12 pC (*solid squares*). Thus, we tested whether long-term treatments with cAMP changed the efficiency of excitation-secretion coupling (*open circles*). Fig. 8 *A* shows that the two ΔC plots are positively correlated with the quantity of charge through statistically indistinguishable linear regressions: 1.6 ± 0.1 fF/pC for controls and 2.0 ± 0.1 fF/pC for cAMP-treated cells ($p > 0.5$). This suggests that long-term cAMP treatments do not alter the efficiency of exocytosis when T- and R-type channels contribute to the total current. The same efficiency was observed when L-type channels were also available. In this case, RCCs were pretreated with ω-toxins and tested in the absence of nifedipine, providing an increased quantity of Ca^{2+} charges which extended the range of linearity of excitation-secretion coupling (*open triangles* in Fig. 8 *B*).

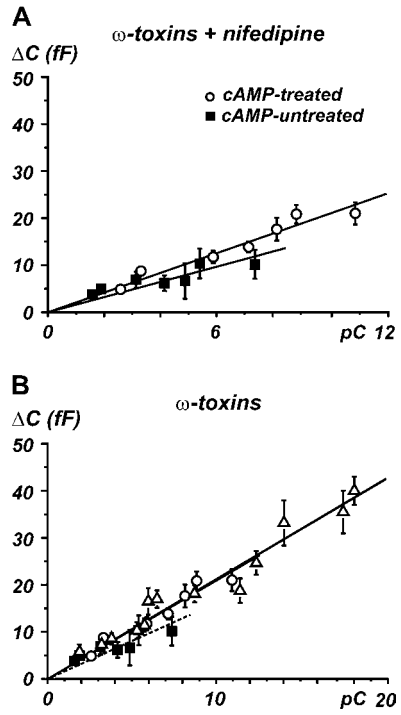

FIGURE 8 T-type channels are coupled to exocytosis with the same efficacy of L- and R-type channels. (*A*) ΔC increases versus the corresponding quantity of charge for cAMP-untreated (R-type channels, ■) and cAMP-treated cells (T- plus R-type channels, ○). Linear regression gave 1.6 ± 0.1 fF/pC and 2.0 ± 0.1 fF/pC, respectively. Cells were pretreated with ω-toxins, and nifedipine was in the bath. (*B*) Ca^{2+} dependence of exocytosis is compared for R-, T-, and L-type channels. Experimental data for cAMP-untreated cells (■) and long-term cAMP-treated cells (○) are the same as in *A*. Data points (△) and linear regression relative to L-type channels are taken from Carabelli et al. (14). Slope of straight line is 2.1 ± 0.1 (fF/pC).

Single exocytic events are unaffected by long-term exposures to cAMP

The contribution of unitary exocytic events was estimated by analyzing the trial-to-trial variations between consecutive depolarization-evoked capacitance increases through a modified procedure of the method described by Moser and Neher (47) and Carabelli et al. (14). A total of ~150 consecutive brief depolarizations (20 ms) at –20 mV were applied at 0.3 Hz and the corresponding capacitance increase ΔC was plotted versus time (Fig. 9, *top*). Typically, the RCCs that displayed sizeable exocytosis had rapid rundown of the secretory response (vesicle depletion) that leveled off to a mean steady-state value after the first 20–25 pulses. The variance of the ''stationary fluctuations'' ($\sigma^2_{\Delta C}$) around the mean ($\langle \Delta C \rangle$) was estimated and used to calculate the size of the single secretory event (Δc) through the equation:

$$\Delta c(1-p) = \sigma^2_{\Delta C}/\langle \Delta C \rangle, \quad (1)$$

which is derived by assuming 1), quantal release with binomial statistics of vesicle release with p indicating the release probability per vesicle, and 2), $\Delta C = N\,\Delta c\,p$ with N indicating the number of vesicles in the IRP (47). Due to the limited Ca^{2+} entry during depolarization p is assumed to be very small (<0.2) and neglected. To compensate for the slow drift of the mean ΔC, the sample variance was calculated versus the averaged sample means of four consecutive ΔC, ''moving bins'' (47). The value of $\sigma^2_{\Delta C}$ was corrected for the background variance of C_m (σ^2_{Cm}), by subtracting σ^2_{Cm} from $\sigma^2_{\Delta C}$. At the conditions of our ΔC measurements obtained by averaging 50 ms segments of C_m before each current pulse (see Materials and Methods), the estimated σ^2_{Cm} was on average 2.5 fF^2 in both cAMP-treated and -untreated cells. Since this value was ~25% $\sigma^2_{\Delta C}$, this implies that regardless of cAMP treatment, not accounting for σ^2_{Cm} would overestimate Δc by ~30%.

Fig. 9 shows the results of the ''stationary fluctuation'' analysis in a typical untreated and cAMP-treated cell (*panels A* and *B*). There is a rapid decay of ΔC in both cases due to vesicle depletion during the first 25 pulses and stationary fluctuations of ΔC around the mean at later pulses. In cAMP-treated cells the mean stationary value was higher due to the contribution of T-type channels, but also the sample variance was higher with respect to control cells, suggesting that Δc does not change significantly during cAMP treatment (1.0 ± 0.2 fF in $n = 8$ control cells and 1.0 ± 0.25 fF in $n = 10$ cAMP-treated cells) (Fig. 9, *inset*). Notice that the present estimate of Δc is in fairly good agreement with the previously reported size of single secretory events estimated using ''nonstationary'' fluctuation analysis in the same preparation (0.9 ± 0.1 fF) (14). This allows concluding that recruitment of T-type channels does not alter the elementary size of single secretory events.

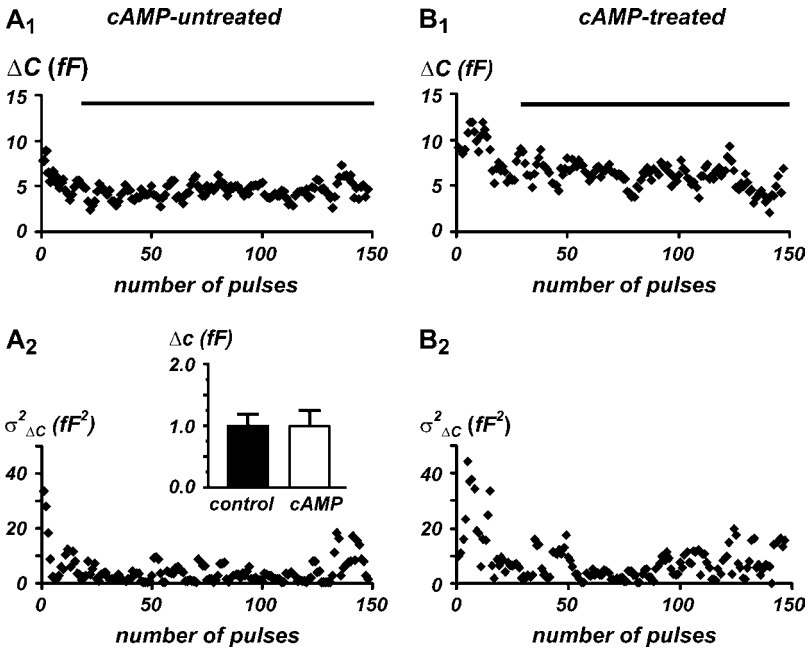

FIGURE 9 Single quantal size is not affected by the long-term cAMP treatment. (A_1 and B_1) ΔC increases in response to 150 consecutive pulse depolarization applied at –20 mV and lasting 20 ms (0.3 Hz), in the absence of (A_1) and after cAMP (B_1) treatment. The horizontal lines indicate the period during which ΔC values were used for calculating the mean quantal size ΔC (see text). (A_2 and B_2) Variances of ΔC increases, evaluated by moving bin analysis. (*Inset*) Mean value of single secretory events (Δc) for control and cAMP-treated cells. ΔC values were calculated from Eq. 1 by subtracting from $\sigma^2_{\Delta C}$ the background variance of C_m (σ^2_{Cm}) that was determined by off-line filtering to 125 Hz the 50 ms baseline noise preceding each ΔC measurement.

DISCUSSION

We have provided evidence that cAMP-recruited T-type channels are effectively coupled to exocytosis in RCCs and that they contribute to secretion with the same efficiency of HVA Ca^{2+} channels (R, L, N, P/Q) commonly expressed in RCCs. As T-type channels contribute to the exocytosis without changing the size of single secretory events and the Ca^{2+} dependence, it is likely that the secretion induced by chronic exposures to cAMP is associated to Ca^{2+} entering through newly recruited T-type channels rather than to downstream changes of the secretory machinery. The net result is an increased fast exocytosis at low voltages associated with a selective increase of functioning T-type channels coupled to secretion.

In our case, 3–5 days exposure to pCPT-cAMP had no effects on the density of HVA Ca^{2+} channels (25), and we checked specifically that long-term cAMP treatments did not alter HVA channel contribution to secretion (Fig. 6). This was of particular importance and furnished convincing evidence that long-term cAMP treatments have totally different effects on Ca^{2+} currents and secretion compared to short-term treatments (1 mM cAMP, 30 min). Short treatments double the secretion and enhance L-type currents by only 20% (14). The increased secretion in this case is attributed to changes of the secretory machinery downstream of Ca^{2+} entry, due to an increased efficiency of release and a doubling of the size of single secretory events.

T-type channels contribute to exocytosis with the same efficiency of other HVA channels

Several lines of evidence indicate that in adult RCCs T-type channels are effectively coupled to secretion: 1), there is strict correlation between the voltage dependence of secretion and Ca^{2+} entry through T-type channels (Fig. 3), 2), Ni^{2+} effectively blocks T-type currents and the associated exocytosis (Fig. 4), and 3), in the presence of Ni^{2+} and ω-toxins, cAMP is unable to affect the secretory response associated with L- and R-type channels. This is in contrast to what is reported in embryonic RCCs in which the α_{1H} T-type channels did not produce secretion (23). The discrepancy could be due to the lack of some critical factor associated to secretion in immature RCCs. Uncoupling cannot certainly depend on the lack of the ''synprint'' site on the α_{1H} subunit (36) that favors the coupling of N- and P/Q-type channels to SNARE proteins (48). In fact, L-type channels, which also do not possess the ''synprint'' site, are effectively coupled to secretion in RCCs (14,16,49,50) and MPC 9/3L cells (33). Alternatively, the uncoupling could be the result of a lower quantity of Ca^{2+} entry associated to a reduced expression density of T-type channels in immature RCCs (6.5 pA/pF at –10 mV in 10 mM Ba^{2+}) versus a higher density in mature cAMP-treated RCCs (10–20 pA/pF; at –10 mV in 10 mM Ca^{2+}) (25) or to differences in the Ca^{2+} buffering system that plays a critical role in chromaffin cells, due to the significant distance at which Ca^{2+} channels are located from release sites (200 nm on average) (17). It is worth noticing, however, that T-type channels are effectively coupled to fast secretion in a number of cell preparations, including melanotropes (31), INS-1 β-cells (29), MPC 9/3L cells (33), and retinal bipolar cells (32), suggesting a constitutive functional role of T-type channels in controlling fast exocytosis in a variety of cells.

Our data clearly show that, similarly to L-type channels (14), the Ca^{2+} dependence of secretion associated with T-type channels is roughly linear and remains unaltered in

RCCs (~2 fF/pC), indicating similar couplings of the two channel types with the secretory apparatus. In relation to this, there are two interesting points worth discussing. First, rough linearity between Ca^{2+} charges and exocytosis is a property of several neuroendocrine cells and some neuronal preparation (for review, see Kits and Mansvelder (46)). Either strict or rough linearity is reported in RCCs (14,16,40), BCCs (45), melanotropes (31), pancreatic β-cells (51), pituitary cells (52), peptidergic nerve terminals (53), and sympathetic ganglia (54). Given this, the second interesting issue to consider is that changes in the steepness of the Ca^{2+} dependence of secretion are usually associated with treatments altering the process of vesicle fusion or vesicle trafficking, which usually affect the size of RRP (or IRP). This includes short-term treatments with cAMP (14), mutations of Rab3A (45), acute application of dopamine (31), depletion of intracellular Ca^{2+} stores (55), and overexpression of tomosyn, a syntaxin-binding protein (56), whereas alteration of channel densities (14,16,46), modulation of channel gating (18), or increments of Ca^{2+} fluxes via Ca^{2+} channel agonists (51) do not alter the slope of Ca^{2+} efficiency of release. Thus, it seems reasonable that recruitment of newly synthesized T-type channels follows the general rule that modifications of Ca^{2+} channel densities do not affect the Ca^{2+} dependence of exocytosis in chromaffin cells.

The vesicle pool, probability of release, and rate of release associated with newly recruited T-type channels

Long-term treatments with cAMP preserve the size of the releasable pool, suggesting that newly recruited T-type channels mobilize vesicles from an IRP comparable to that controlled by HVA channels. We proved this by using the conventional double-pulse protocol (42), which furnished an IRP significantly higher than that estimated with single pulses of increasing duration (36 fF vs. 21 fF; Fig. 7, *B* and *D*). As the former can be considered an overestimate and the latter an underestimate, the true IRP is reasonably expected around 30 fF, which is a value comparable with the IRP controlled by HVA channels in RCCs (34 and 40 fF) (14,40) and mouse chromaffin cells (MCCs) (47 fF) (57). A second important consideration is that T-type channels do not alter the high probability of vesicle release with pulses of 100 ms (p ~0.6). Similar values of p are reported in RCCs (14), BCCs (42), and MCCs (57) when L-, N-, and P/Q-type channels are the only Ca^{2+} channels available. In line with this, it is worth noticing that T-type channels induce remarkably fast exocytosis with a high initial rate of release (466 fF/s), which is only partially smaller than the rate associated with HVA channels in the same cell preparation (580 and 680 fF/s) (14,40). However, if as suggested (40) the rate of exocytosis depends on Ca^{2+} channel density, the lower density of T-type channels with respect to HVA channels largely justifies the lower rate in cAMP-treated RCCs (see below).

Having shown that T-type channels effectively contribute to the depletion of immediately releasable vesicles, it cannot be excluded that they also contribute to the release of the larger RRP of vesicles that is defined as the pool of all release competent vesicles estimated using photorelease of caged-Ca or prolonged and repeated depolarizations. In RCCs the RRP is estimated to be ~10 times the size of the IRP (330 fF; see Horrigan and Bookmann (40)), whereas in MCCs, more recent estimates using caged-Ca compounds have set the size of IRP and RRP at 47 and 205 fF, respectively (57). As the RRP is largely depleted during repeated stimulations lasting several hundreds of milliseconds, it is likely that even if T-type channels are associated with this pool of vesicles their contribution would rapidly vanish given their fast and complete inactivation with pulses longer than 100 ms (58). This peculiarity reinforces the notion that a major role for T-type channels is in the control of a small pool of vesicles related to fast exocytosis and associated with transient Ca^{2+} injections of 20 to 50 ms.

A final point worth considering is that the density of T-type channels would hardly alter the overall arrangement of Ca^{2+} channels controlling secretion in RCCs, assuming that the channels will be uniformly distributed along the cell surface. In fact, from the peak current (Ip = 160 pA at −10 mV in 10 mM Ca^{2+}; E_{Ca} = +70 mV) (25), the single-channel conductance (γ = 1 pS), the probability of channel opening (p = 0.5) (58), and the mean cell diameter (18 μm after 4 days in culture) we estimated a density of ~4 channels/μm^2 for T-type channels, which is smaller than the HVA channel density (6 channels/μm^2) derived from the data of Cesetti et al. (27) (Ip = 300 pA at +20 mV in 10 mM Ca^{2+}, E_{Ca} = +70 mV) with γ = 2 pS and p = 0.5. This implies that channel density would increase from 6 to 10 channels/μm^2 when the two channel types contribute simultaneously to secretion (between –10 and +40 mV), but it would be limited to four channels/μm^2 at lower voltages (from –50 to –10 mV) when the T-type is the only channel controlling secretion. Indeed, accounting for the driving force and for the 50% lower ion conductance of T-type channels, the contribution of these channels to the total current at +20 mV is ~1/3 of that carried by the HVA channels. Thus, it appears that newly recruited T-type channels do not produce major changes to the overall distribution of voltage-gated Ca^{2+} channels controlling secretion except that by activating at lower voltages they can initiate exocytosis at potentials near resting conditions.

CONCLUSIONS

Long-term incubation with cAMP clearly has very different consequences on the secretory response of RCCs compared with the acute treatments: brief exposure to pCPT-cAMP (1 mM, 30 min) causes a 100% increase of the secretory response attributed to an increased IRP and a doubling of the size of single secretory events (14). Unlike the short-term

incubation, the long-term treatment preserves the size of IRP and single secretory events. Interestingly, 3 days treatment with cAMP also increases the quantity of released catecholamines per vesicle (59), suggesting increased concentrations of adrenaline and noradrenaline within the secretory granules.

Although understanding the physiological consequences of recruiting T-type channels and their related secretion is beyond the purpose of this work, it is worth noticing that upregulation of low-threshold channels and ''low-threshold exocytosis'' in RCCs may have drastic effects on cell excitability and adrenal gland function. In fact, even though long-term cAMP treatments do not alter the frequency of action potential generation during bursts, recruitment of T-type channels significantly lowers the firing threshold in RCCs (25). This could possibly increase the number of action potential bursts that appears to be one of the most critical parameters regulating secretion in RCCs (60). In addition to that, a sizeable ''low-threshold secretion'' as reported here may help increase the release of catecholamines during sustained cell activity. Under these circumstances, cAMP levels are likely to remain elevated for long periods of time due to the positive feedback that originates from the increased release of catecholamines (59) and the activation of β_1-adrenoreceptors expressed in RCCs (27).

We thank Dr. C. Franchino for preparing the cell cultures.

This work was supported by the Italian MIUR (grant COFIN No. 2005054435 to E.C.), the Regione Piemonte (grants No. A28-2005 to V.C. and No. D14-2005 to E.C.), and the San Paolo IMI Foundation (grant to the NIS Center of Excellence).

REFERENCES

1. Albillos, A., A. R. Artalejo, M. G. Lopez, L. Gandía, A. G. García, and E. Carbone. 1994. Calcium channel subtypes in cat chromaffin cells. *J. Physiol.* 477:197–213.
2. Albillos, A., A. G. García, B. Olivera, and L. Gandía. 1996. Re-evaluation of the P/Q Ca^{2+} channel components of Ba^{2+} currents in bovine chromaffin cells superfused with solutions containing low and high Ba^{2+} concentrations. *Pflugers Arch.* 432:1030–1038.
3. Albillos, A., A. G. García, and L. Gandía. 1993. ω-Agatoxin-IVA-sensitive calcium channels in bovine chromaffin cells. *FEBS Lett.* 336:259–262.
4. Bossu, J. L., M. De Waard, and A. Feltz. 1991. Two types of calcium channels are expressed in adult bovine chromaffin cells. *J. Physiol.* 437:621–634.
5. Bossu, J. L., M. De Waard, and A. Feltz. 1991. Inactivation characteristics reveal two calcium currents in adult bovine chromaffin cells. *J. Physiol.* 437:603–620.
6. Hoshi, T., and S. J. Smith. 1987. Large depolarization induces long openings of voltage-dependent calcium channels in adrenal chromaffin cells. *J. Neurosci.* 7:571–580.
7. Lomax, R. B., P. Michelena, L. Nunez, J. Garcia-Sancho, A. G. García, and C. Montiel. 1997. Different contributions of L- and Q-type Ca2+ channels to Ca^{2+} signals and secretion in chromaffin cell subtypes. *Am. J. Physiol.* 272:C476–C484.
8. Lopez, M. G., M. Villarroya, B. Lara, R. Martinez Sierra, A. Albillos, A. G. García, and L. Gandía. 1994. Q- and L-type Ca^{2+} channels dominate the control of secretion in bovine chromaffin cells. *FEBS Lett.* 349:331–337.
9. O'Farrell, M., and P. D. Marley. 2000. Differential control of tyrosine hydroxylase activation and catecholamine secretion by voltage-operated Ca^{2+} channels in bovine chromaffin cells. *J. Neurochem.* 74: 1271–1278.
10. Albillos, A., E. Neher, and T. Moser. 2000. R-type Ca^{2+} channels are coupled to the rapid component of secretion in mouse adrenal slice chromaffin cells. *J. Neurosci.* 20:8323–8330.
11. Artalejo, C. R., M. E. Adams, and A. P. Fox. 1994. Three types of Ca^{2+} channel trigger secretion with different efficacies in chromaffin cells. *Nature.* 367:72–76.
12. Lara, B., L. Gandía, R. Martinez-Sierra, A. Torres, and A. G. García. 1998. Q-type Ca^{2+} channels are located closer to secretory sites than L-type channels: functional evidence in chromaffin cells. *Pflugers Arch.* 435:472–478.
13. Carabelli, V., I. Carra, and E. Carbone. 1998. Localized secretion of ATP and opioids revealed through single Ca2+ channel modulation in bovine chromaffin cells. *Neuron.* 20:1255–1268.
14. Carabelli, V., A. Giancippoli, P. Baldelli, E. Carbone, and A. R. Artalejo. 2003. Distinct potentiation of L-type currents and secretion by cAMP in rat chromaffin cells. *Biophys. J.* 85:1326–1337.
15. Mansvelder, H. D., and K. S. Kits. 1998. The relation of exocytosis and rapid endocytosis to calcium entry evoked by short repetitive depolarizing pulses in rat melanotropic cells. *J. Neurosci.* 18:81–92.
16. Kim, S. J., W. Lim, and J. Kim. 1995. Contribution of L- and N-type calcium currents to exocytosis in rat adrenal medullary chromaffin cells. *Brain Res.* 675:289–296.
17. Klingauf, J., and E. Neher. 1997. Modelling buffered Ca^{2+} diffusion near the membrane: implications for secretion in neuroendocrine cells. *Biophys. J.* 72:674–690.
18. Ulate, G., S. R. Scott, J. Gonzalez, J. A. Gilabert, and A. R. Artalejo. 2000. Extracellular ATP regulates exocytosis in inhibiting multiple Ca^{2+} channel types in bovine chromaffin cells. *Pflugers Arch.* 439: 304–314.
19. Lukyanetz, E. A., and E. Neher. 1999. Different types of calcium channels and secretion from bovine chromaffin cells. *Eur. J. Neurosci.* 11:2865–2873.
20. Villarroya, M., R. Olivares, A. Ruiz, M. F. Cano-Abad, R. de Pascual, R. B. Lomax, M. G. Lopez, I. Mayorgas, L. Gandía, and A. G. García. 1999. Voltage inactivation of Ca^{2+} entry and secretion associated with N- and P/Q-type but not L-type Ca^{2+} channels of bovine chromaffin cells. *J. Physiol.* 516:421–432.
21. Gil, A., S. Viniegra, P. Neco, and L. M. Gutierrez. 2001. Co-localization of vesicles and P/Q Ca^{2+}-channels explains the preferential distribution of exocytotic active zones in neurites emitted by bovine chromaffin cells. *Eur. J. Cell Biol.* 80:358–365.
22. Garcia-Palomero, E., I. Cuchillo-Ibanez, A. G. García, J. Renart, A. Albillos, and C. Montiel. 2000. Greater diversity than previously thought of chromaffin cell Ca^{2+} channels, derived from mRNA identification studies. *FEBS Lett.* 481:235–239.
23. Bournaud, R., J. Hidalgo, H. Yu, E. Jaimovich, and T. Shimar. 2001. Low threshold T-type calcium current in rat chromaffin cells. *J. Physiol.* 537:35–44.
24. Hollins, B., and S. R. Ikeda. 1996. Inward currents underlying action potentials in rat adrenal chromaffin cells. *J. Neurophysiol.* 76:1195–1211.
25. Novara, M., P. Baldelli, D. Cavallari, V. Carabelli, A. Giancippoli, and E. Carbone. 2004. Exposure to cAMP and beta-adrenergic stimulation recruits Ca(V)3 T-type channels in rat chromaffin cells through Epac cAMP-receptor proteins. *J. Physiol.* 558:433–449.
26. Carabelli, V., J. M. Hernandez-Guijo, P. Baldelli, and E. Carbone. 2001. Direct autocrine inhibition and cAMP-dependent potentiation of single L-type Ca^{2+} channels in bovine chromaffin cells. *J. Physiol.* 532:73–90.
27. Cesetti, T., J. M. Hernandez-Gujio, P. Baldelli, V. Carabelli, and E. Carbone. 2003. Opposite action of β1- and β2-adrenergic receptors on Ca(V)1 L-channel current in rat adrenal chromaffin cells. *J. Neurosci.* 23:73–83.

28. Schrier, A. D., H. Wang, E. M. Talley, E. Perez-Reyes, and P. Q. Barrett. 2001. Alpha1H T-type Ca2+ channel is the predominant subtype expressed in bovine and rat zona glomerulosa. *Am. J. Physiol. Cell Physiol.* 280:C265–C272.

29. Bhattacharjee, A., R. M. Whitehurst, M. Zhang, L. Wang, and M. Li. 1997. T-type calcium channels facilitate insulin secretion by enhancing general excitability in the insulin-secreting beta-cell line. *Endocrinology.* 138:3735–3740.

30. Leuranguer, V., A. Monteil, E. Bourinet, G. Dayanithi, and J. Nargeot. 2000. T-type calcium currents in rat cardiomyocytes during postnatal development: contribution to hormone secretion. *Am. J. Physiol. Heart Circ. Physiol.* 279:H2540–H2548.

31. Mansvelder, H. D., J. C. Lodder, M. S. Sons, and K. S. Kits. 2002. Dopamine modulates exocytosis independent of Ca(2+) entry in melanotropic cells. *J. Neurophysiol.* 87:793–801.

32. Pan, Z. H., H. J. Hu, P. Perring, and R. Andrade. 2001. T-type Ca^{2+} channels mediate neurotransmitter release in retinal bipolar cells. *Neuron.* 32:89–98.

33. Harkins, A. B., A. L. Cahill, J. F. Powers, A. S. Tischler, and A. P. Fox. 2003. Expression of recombinant calcium channels support secretion in a mouse pheochromocytoma cell line. *J. Neurophysiol.* 90:2325–2333.

34. Rae, J., K. Cooper, P. Gates, and M. Watsky. 1991. Low access resistance perforated patch recordings using amphotericin B. *J. Neurosci. Methods.* 37:15–26.

35. Barry, P. H., and J. W. Lynch. 1991. Liquid junction potentials and small cell effects in patch-clamp analysis. *J. Membr. Biol.* 121:101–117.

36. Cribbs, L. L., J. H. Lee, J. Yang, J. Satin, Y. Zhang, A. Daud, J. Barclay, M. P. Williamson, M. Fox, M. Rees, and E. Perez-Reyes. 1998. Cloning and characterization of alpha1H from human heart, a member of the T-type Ca^{2+} channel gene family. *Circ. Res.* 83:103–109.

37. Lee, J. H., J. C. Gomora, L. L. Cribbs, and E. Perez-Reyes. 1999. Nickel block of three cloned T-type calcium channels: low concentrations selectively block alpha1H. *Biophys. J.* 77:3034–3042.

38. Hwang, O., M. L. Kim, and J. D. Lee. 1994. Differential induction of gene expression of catecholamine biosynthetic enzymes and preferential increase in norepinephrine by forskolin. *Biochem. Pharmacol.* 48: 1927–1934.

39. Newcomb, R., B. Szoke, A. Palma, G. Wang, X. Chen, W. Hopkins, R. Cong, J. Miller, L. Urge, K. Tarczy-Hornoch, J. A. Loo, D. J. Dooley, L. Nadasdi, R. W. Tsien, J. Lemos, and G. Miljanich. 1998. Selective peptide antagonist of the class E calcium channel from the venom of the tarantula Hysterocrates gigas. *Biochemistry.* 37:15353–15362.

40. Horrigan, F. T., and R. J. Bookmann. 1994. Releasable pools and the kinetics of exocytosis in adrenal chromaffin cells. *Neuron.* 13:1119–1129.

41. Zamponi, G. W., E. Bourinet, and T. P. Snutch. 1996. Nickel block of a family of neuronal calcium channels: subtype- and subunit-dependent action at multiple sites. *J. Membr. Biol.* 151:77–90.

42. Gillis, K. D., R. Mossner, and E. Neher. 1996. Protein kinase C enhances exocytosis from chromaffin cells by increasing the size of the readily releasable pool of secretory granules. *Neuron.* 16:1209–1220.

43. Klöckner, U., J.-H. Lee, L. L. Cribbs, A. Daud, J. Hescheler, A. Pereverzev, E. Perez-Reyes, and T. Schneider. 1999. Comparison of the Ca^{2+} currents induced by expression of three cloned alpha1 subunits, alpha1G, alpha1H and alpha1I, of low-voltage-activated T-type Ca^{2+} channels. *Eur. J. Neurosci.* 11:4171–4178.

44. Moser, T., and E. Neher. 1997. Rapid exocytosis in single chromaffin cells recorder from mouse adrenal slices. *J. Neurosci.* 17:2314–2323.

45. Thiagarajan, R., T. Tewolde, Y. Li, P. L. Becker, M. M. Rich, and K. L. Engisch. 2004. Rab3A negatively regulates activity-dependent modulation of exocytosis in bovine adrenal chromaffin cells. *J. Physiol.* 555:439–457.

46. Kits, K. S., and H. D. Mansvelder. 2000. Regulation of exocytosis in neuroendocrine cells: spatial organization of channels and vesicles, stimulus-secretion coupling, calcium buffers and modulation. *Brain Res. Brain Res. Rev.* 33:78–94.

47. Moser, T., and E. Neher. 1997. Estimation of mean exocytic vesicle capacitance in mouse adrenal chromaffin cells. *Proc. Natl. Acad. Sci. USA.* 94:6735–6740.

48. Catterall, W. A. 2000. Structure and regulation of voltage-gated Ca^{2+} channels. *Annu. Rev. Cell Dev. Biol.* 16:521–555.

49. Baldelli, P., J. M. Hernandez-Guijo, V. Carabelli, M. Novara, T. Cesetti, E. Andres-Mateos, C. Montiel, and E. Carbone. 2004. Direct and remote modulation of L-channels in chromaffin cells: distinct actions on alpha1C and alpha1D subunits? *Mol. Neurobiol.* 29:73–96.

50. Lim, W., S. J. Kim, H. D. Yan, and J. Kim. 1997. Ca2+-channel-dependent and -independent inhibition of exocytosis by extracellular ATP in voltage-clamped rat adrenal chromaffin cells. *Pflugers Arch.* 435:34–42.

51. Barg, S., X. Ma, L. Eliasson, J. Galvanovskis, S. O. Gopel, S. Obermuller, J. Platzer, E. Renstrom, M. Trus, D. Atlas, J. Striessnig, and P. Rorsman. 2001. Fast exocytosis with few Ca(2+) channels in insulin-secreting mouse pancreatic B cells. *Biophys. J.* 81:3308–3323.

52. Hsu, S. F., and M. B. Jackson. 1996. Rapid exocytosis and endocytosis in nerve terminals of the rat posterior pituitary. *J. Physiol.* 494:539–553.

53. Seward, E. P., N. I. Chernevskaya, and M. C. Nowycky. 1995. Exocytosis in peptidergic nerve terminals exhibits two calcium-sensitive phases during pulsatile calcium entry. *J. Neurosci.* 15: 3390–3399.

54. Peng, Y. Y., and R. S. Zucker. 1993. Release of LHRH is linearly related to the time integral of presynaptic Ca2+ elevation above a threshold level in bullfrog sympathetic ganglia. *Neuron.* 10:465–473.

55. Fomina, A. F., and M. C. Nowycky. 1999. A current activated on depletion of intracellular Ca2+ stores can regulate exocytosis in adrenal chromaffin cells. *J. Neurosci.* 19:3711–3722.

56. Yizhar, O., U. Matti, R. Melamed, Y. Hagalili, D. Bruns, J. Rettig, and U. Ashery. 2004. Tomosyn inhibits priming of large dense-core vesicles in a calcium-dependent manner. *Proc. Natl. Acad. Sci. USA.* 101:2578–2583.

57. Voets, T., E. Neher, and T. Moser. 1999. Mechanisms underlying phasic and sustained secretion in chromaffin cells from mouse adrenal slices. *Neuron.* 23:607–615.

58. Carbone, E., and H. D. Lux. 1987. Single low-voltage-activated calcium channels in chick and rat sensory neurons. *J. Physiol.* 386: 571–601.

59. Tang, K. S., A. Tse, and F. W. Tse. 2005. Differential regulation of multiple populations of granules in rat adrenal chromaffin cells by culture duration and cyclic AMP. *J. Neurochem.* 92:1126–1139.

60. Duan, K., X. Yu, C. Zhang, and Z. Zhou. 2003. Control of secretion by temporal patterns of action potentials in adrenal chromaffin cells. *J. Neurosci.* 23:11235–11243.